Research Square

Preprints are preliminary reports that have not undergone peer review.
They should not be considered conclusive, used to inform clinical practice,
or referenced by the media as validated information.

Stochastic SIS Model with Dynamic Node Activity: Epidemic Threshold and Stationary States

Alexey V. Nikiforov

alva.nikiforov@svfu.ru

M.~K. Ammosov North-Eastern Federal University

Alexey A. Magazev

Omsk State Technical University

Research Article

Keywords:

Posted Date: October 29th, 2026

DOI: https://doi.org/10.21203/rs.3.rs-11377986/v1

License: This work is licensed under a Creative Commons Attribution 4.0 International License.
Read Full License

Additional Declarations: No competing interests reported.

Stochastic SIS Model with Dynamic Node Activity: Epidemic Threshold and Stationary States

Alexey V. Nikiforov[1*] and Alexey A. Magazev[2]

[1*]M. K. Ammosov North-Eastern Federal University, Yakutsk, Russia.
[2]Omsk State Technical University, Omsk, Russia.

*Corresponding author(s). E-mail(s): alva.nikiforov@svfu.ru;
Contributing authors: magazev@omgtu.ru;

Abstract

This paper develops and evaluates a stochastic model of infection spreading on a graph with dynamic node activity. Each node is characterized by an epidemiological state (susceptible or infected) and an activity state (enabled or disabled). Only enabled nodes participate in transmission, while the network topology remains fixed. The infection probability of an enabled susceptible node is proportional to its degree and to the fraction of infected nodes among the enabled ones. The continuum analogue of the model is derived in the mean-field approximation and its stationary states are analyzed. Both the epidemic threshold and the stationary infection level coincide with the classical SIS results and are independent of the activity parameter in the symmetric case. The activity parameter therefore affects only the transient dynamics: both the decay of the infection in the subcritical regime and the convergence to the stationary state in the supercritical regime slow down as the activity rate increases. This slowdown is explained by the fact that recovery is possible only for enabled nodes, so that infected nodes temporarily excluded from transmission act as a reservoir that sustains the infection. The results extend the classical mean-field SIS model to the case of dynamic node availability.

Keywords: computer virus propagation, stochastic modeling, epidemic model, node activity, Erdős–Rényi graph, mean-field approximation

1 Introduction

The mathematical modeling of spreading processes in networks has become a standard tool in many disciplines. Its applications range from the classical epidemiology of infectious diseases [1] to the propagation of rumors and misinformation in social networks [2, 3], the spread of malware and computer viruses in communication systems [4, 5], and the diffusion of ideas or behaviors in online communities [6, 7]. In all these cases, the process can be described in terms of a network of interacting units, each of which occupies one of several possible states, and transitions between the states occur according to probabilistic rules. This common structure has motivated the development of a unified framework based on graph theory and stochastic processes [8], which is now widely used in mathematical biology, sociology, and computer science.

Among the mathematical tools used to describe spreading processes, compartmental epidemic models occupy a central place. In the classical SIS model, each individual is either susceptible or infected, and the dynamics is governed by the balance between infection and recovery. The SIR model introduces an additional recovered state, while more complex models include exposed or asymptomatic compartments. A key characteristic of all these models is the existence of a threshold parameter, usually expressed through the basic reproduction number $\mathcal{R}_0$, which separates the regimes of extinction and persistence of the infection.

When the population is structured as a network, the threshold behavior is modified by the topology [8]. The mean-field analysis of the SIS model on networks shows that the epidemic threshold is determined by the spectral properties of the adjacency matrix, and in the case of uncorrelated networks it is expressed through the first two moments of the degree distribution. This result, obtained by Pastor-Satorras and Vespignani [1], demonstrated that the epidemic threshold can vanish in the limit of infinite scale-free networks, which has important implications for the spread of infections in heterogeneous populations.

In many real systems, however, the structure of the network is not static: contacts between individuals are established and broken over time. Typical examples include communication networks in which workstations are periodically switched off, mobile networks in which devices move in and out of range, and social networks in which the set of active contacts changes over time. This observation has led to the development of *temporal networks*, in which the edges are active only during certain time intervals [9]. A related class of models, known as activity-driven networks, describes the temporal evolution of contacts through the activity of individual nodes [10]. In both cases, the temporal structure of interactions strongly affects the dynamics of spreading processes.

Despite these advances, most existing models assume that either the edges or the nodes are continuously available for transmission. In many practical settings, however, the nodes themselves switch between active and inactive states, while the underlying communication network remains fixed. This is typical, for example, of devices that periodically go offline, or of individuals who are not always available for contact. In this work, we propose and analyze a stochastic SIS model in which each node is characterized by an activity state, and only active nodes participate in the transmission process. Our goal is to derive the mean-field equations for the model, to identify

the epidemic threshold, and to quantify the effect of the activity parameter on the dynamics of the infection.

The paper is organized as follows. In Section 2, we introduce the stochastic model and specify the transition rules. In Section 3, we derive the mean-field approximation and analyze the stationary states and their stability. Section 4 describes the simulation algorithm, and Section 5 presents the results of the numerical experiments. Finally, we summarize the main findings and outlines possible directions for future work.

2 Mathematical Model

We consider the spread of malicious software in a computer network modeled as a connected undirected graph $G = (V, L)$, where $V = \{1, \ldots, N\}$ is the set of nodes and L is the set of edges representing possible communication links. Each node $a \in V$ is characterized by two independent binary attributes: an activity state (D or E) and an epidemiological state (I or S), where D and E denote *disabled* and *enabled* states, and S and I denote *susceptible* and *infected* states. Thus, each node can be in one of four states: (D, S), (D, I), (E, S), and (E, I). Only enabled nodes participate in the transmission process: a disabled node retains its epidemiological state but does not spread the infection.

Time is discrete: $t = 0, 1, 2, \ldots$. At each step, all nodes update their states simultaneously according to the probabilistic rules described below. All transition probabilities are defined per step.

Let $DS(t)$, $DI(t)$, $ES(t)$, and $EI(t)$ denote the number of nodes in the corresponding states at time t. Since each node is in exactly one state,

$$DS(t) + DI(t) + ES(t) + EI(t) = N.$$

We also introduce the total number of enabled nodes, the total number of infected nodes, and the fraction of infected nodes among the enabled ones:

$$E(t) = ES(t) + EI(t), \qquad I(t) = DI(t) + EI(t), \qquad i(t) = \frac{EI(t)}{E(t)}.$$

The quantity $i(t)$ determines the infection pressure exerted by the enabled part of the network and plays a central role in the model.

The dynamics of a node are governed by two types of transitions: changes in its activity state and changes in its epidemiological state. Activity changes are independent of the epidemiological status: a disabled node can become enabled, and an enabled node can become disabled. In contrast, epidemiological transitions depend on the current activity state. An enabled susceptible node can become infected; an enabled infected node can recover and become susceptible again. A disabled node cannot change its epidemiological state: a disabled infected node does not recover, and a disabled susceptible node does not become infected while it remains disabled.

Let λ_+ and λ_- denote the probabilities that a disabled node becomes enabled and that an enabled node becomes disabled during one step, respectively. Let δ be the probability that an enabled infected node recovers during one step, and μ_a be the

probability that an enabled susceptible node a becomes infected during one step. In contrast to the activity and recovery probabilities, which are the same for all nodes, μ_a depends on the relative connectivity of node a: nodes with a larger number of links are more likely to become infected. All parameters take values in $[0, 1]$. Since epidemiological transitions occur only if the node remains enabled after the activity update, the effective probabilities of infection and recovery are $(1 - \lambda_-)\mu_a$ and $(1 - \lambda_-)\delta$, respectively. The transition probabilities are summarized in Fig. 1; the probabilities of remaining in the same state follow from the normalization condition.

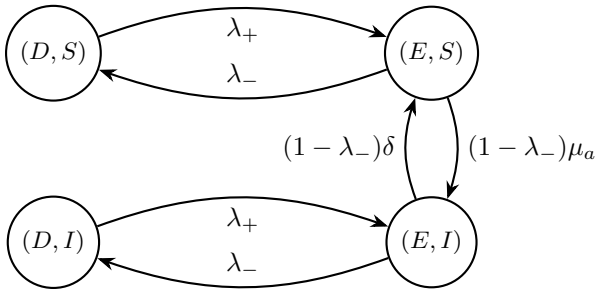

Fig. 1 State transition graph of the model for a single node a. Arrows indicate the allowed transitions: activity changes (λ_+, λ_-), infection ($(1 - \lambda_-)\mu_a$), and recovery ($(1 - \lambda_-)\delta$).

To complete the formulation of the model, we need to specify the dependence of the infection probability μ_a on the node index a and on the characteristics of the graph.

In the classical model of Kephart and White [11], the infection probability is assumed to be the same for all nodes and proportional to the infection pressure: $\mu = \beta \langle k \rangle i$, where β is the transmission probability and $\langle k \rangle$ is the average degree of a node. This formulation corresponds to a homogeneous network in which all nodes have the same connectivity and are equally exposed to infection. Another drawback of this formula is that the resulting probability can exceed unity. This issue was addressed by Billings et al. [12], who proposed a more accurate expression based on the probability of being infected by at least one of the infected nodes in the network:

$$\mu = 1 - (1 - \beta \langle k \rangle i)^{Ni},$$

where Ni is the total number of infected nodes. The applicability of this model to real e-mail graphs was analyzed in [13], where the analytical predictions were compared with simulation results for various epidemic parameters. This expression remains bounded between zero and one and is valid for arbitrary i and $\beta \langle k \rangle$. However, it still assumes that all nodes are identical and that the network is homogeneous.

In contrast to the model of Billings et al. [12], where a susceptible node can be infected by any of the infected nodes in the network, in the proposed model infection is transmitted only by the neighbors of the node. This corresponds to the degree-based mean-field approach [14], in which the infection risk is determined by the node degree k_a and by the fraction of infected nodes among the active ones, $i(t)$. The exact

infection probability, under the assumption that transmission events along different links are independent, has the form

$$\mu_a(t) = 1 - \big(1 - \beta\, i(t)\big)^{k_a}.$$

In what follows, we use the linear approximation

$$\mu_a(t) \approx \beta\, k_a\, i(t), \tag{1}$$

which is valid for $\beta\, i(t) \ll 1$. This approximation is used consistently both in the mean-field analysis and in the stochastic simulations.

3 Mean-Field Approximation

The stochastic model described in Section 2 does not admit a simple analytical treatment. To gain insight into its long-term behavior, we consider its continuous-time mean-field analogue, in which all nodes are assumed to be statistically equivalent and the dynamics is described by the fractions of nodes in each state.

Let

$$s_D(t) = \frac{DS(t)}{N}, \quad i_D(t) = \frac{DI(t)}{N}, \quad s_E(t) = \frac{ES(t)}{N}, \quad i_E(t) = \frac{EI(t)}{N}$$

denote the fractions of nodes in states (D, S), (D, I), (E, S), and (E, I), respectively. By definition,

$$s_D(t) + i_D(t) + s_E(t) + i_E(t) = 1.$$

The fraction of infected nodes among the enabled ones is

$$i(t) = \frac{i_E(t)}{s_E(t) + i_E(t)}.$$

In the mean-field approximation, the node-dependent infection probability (1) is replaced by its average over the degree distribution. For small βi, this average reduces to

$$\langle \mu_a \rangle \approx \beta \langle k \rangle i,$$

where $\langle k \rangle$ is the mean degree of the graph. This approximation neglects the structural heterogeneity of nodes and allows the dynamics to be described by a single set of equations for the fractions s_D, i_D, s_E, i_E. The dynamics of these fractions is governed by the balance between incoming and outgoing transitions. Interpreting the per-step probabilities of Section 2 as transition rates, we obtain

$$\frac{ds_D}{dt} = \lambda_- s_E - \lambda_+ s_D, \tag{2}$$

$$\frac{di_D}{dt} = \lambda_- i_E - \lambda_+ i_D, \tag{3}$$

$$\frac{ds_E}{dt} = \lambda_+ s_D + (1-\lambda_-)\delta\, i_E - \lambda_- s_E - (1-\lambda_-)\beta\langle k\rangle i s_E, \tag{4}$$

$$\frac{di_E}{dt} = (1-\lambda_-)\beta\langle k\rangle i s_E + \lambda_+ i_D - \big(\lambda_- + (1-\lambda_-)\delta\big) i_E. \tag{5}$$

The nonlinearity of the system arises from the term $\beta\langle k\rangle i s_E$, which couples the infection pressure $i(t)$ with the fraction of susceptible enabled nodes.

The stationary states of system (2)–(5) are obtained by setting all time derivatives to zero. Solving the resulting algebraic system yields two solutions.

The first solution is the *infection-free state*

$$s_D^* = \frac{\lambda_-}{\lambda_+ + \lambda_-}, \quad i_D^* = 0, \quad s_E^* = \frac{\lambda_+}{\lambda_+ + \lambda_-}, \quad i_E^* = 0. \tag{6}$$

In this state, there are no infected nodes, and the fractions of enabled and disabled nodes are determined solely by the balance between activation and deactivation.

The second solution describes an *endemic state*, in which a finite fraction of enabled nodes remains infected. The corresponding stationary values are

$$s_E^* = \frac{\lambda_+}{\lambda_+ + \lambda_-} \cdot \frac{1}{\mathcal{R}_0}, \quad i_E^* = \frac{\lambda_+}{\lambda_+ + \lambda_-}\left(1 - \frac{1}{\mathcal{R}_0}\right), \tag{7}$$

$$s_D^* = \frac{\lambda_-}{\lambda_+ + \lambda_-} \cdot \frac{1}{\mathcal{R}_0}, \quad i_D^* = \frac{\lambda_-}{\lambda_+ + \lambda_-}\left(1 - \frac{1}{\mathcal{R}_0}\right), \tag{8}$$

where we have introduced the basic reproduction number $\mathcal{R}_0 = \beta\langle k\rangle/\delta$.

The stability of the two stationary solutions can be analyzed by linearizing system (2)–(5) around each equilibrium.

Theorem 1 (Stability of stationary states) *Consider system (2)–(5) with $0 < \lambda_- < 1$, $\lambda_+ > 0$, $\beta > 0$, $\delta > 0$, and $\langle k\rangle > 0$. Then the following statements hold:*

1. *If $\mathcal{R}_0 < 1$, the system has only the infection-free stationary state (6), and this state is locally asymptotically stable.*
2. *If $\mathcal{R}_0 > 1$, the system has two stationary states: the infection-free state (6), which is unstable, and the endemic state (7), (8), which is locally asymptotically stable.*
3. *At $\mathcal{R}_0 = 1$, the two stationary states coincide, and the system undergoes a transcritical bifurcation.*

Proof The stability of each stationary state is determined by the roots of the characteristic polynomial of the Jacobian evaluated at that state. In both cases, the characteristic polynomial factors as

$$\chi(\alpha) = \alpha(\alpha + \lambda_- + \lambda_+)(\alpha^2 + b_1\alpha + b_0),$$

where the zero eigenvalue corresponds to the conservation of the normalization $s_D + i_D + s_E + i_E = 1$, and the eigenvalue $-\lambda_- - \lambda_+$ is always negative. The remaining two eigenvalues are the roots of the quadratic factor; by the Vieta relations, they have negative real parts if

and only if $b_1 > 0$ and $b_0 > 0$. For the infection-free state, these conditions reduce to $\mathcal{R}_0 < 1$; for the endemic state, they reduce to $\mathcal{R}_0 > 1$. Hence the two states exchange stability at $\mathcal{R}_0 = 1$. □

Remark 1 *The transcritical bifurcation at $\mathcal{R}_0 = 1$ is a consequence of the bilinear infection term combined with linear recovery. The activity parameters λ_+ and λ_- affect the position of the endemic state but do not change the threshold value.*

It is instructive to compare the obtained results with the classical SIS model on a static network. In the limit $\lambda_+ = \lambda_- = 0$, the activity state of each node is fixed, and if all nodes are initially enabled, the fractions of disabled nodes vanish:

$$s_D = i_D = 0, \qquad s_E + i_E = 1.$$

The system (2)–(5) then reduces to

$$\frac{di_E}{dt} = \beta\langle k\rangle(1 - i_E)i_E - \delta i_E,$$

whose exact solution is

$$i_E(t) = \frac{i^* i_0}{i_0 + (i^* - i_0)e^{-(\beta\langle k\rangle - \delta)t}}, \qquad i^* = 1 - \frac{1}{\mathcal{R}_0}. \tag{9}$$

In this case, the classical epidemic threshold is [14]

$$\mathcal{R}_0 = \frac{\beta\langle k\rangle}{\delta} = 1.$$

Thus, the threshold obtained above coincides with the well-known mean-field SIS result. The novelty of the present model is that the same threshold is preserved in the presence of dynamic node activity, while the position of the endemic state is modified by the activity parameters.

In summary, the mean-field analysis of the stochastic model yields three main results. First, the system admits two stationary states: the infection-free state and the endemic state, the latter existing only when $\mathcal{R}_0 > 1$. Second, the stability analysis shows that the two states exchange stability at the epidemic threshold $\mathcal{R}_0 = 1$, which corresponds to a transcritical bifurcation. Third, the threshold value $\mathcal{R}_0 = \beta\langle k\rangle/\delta$ does not depend on the activity parameters λ_+ and λ_-, whereas the position of the endemic state does. These analytical predictions will be compared with the results of stochastic simulations in the next section.

4 Simulation Algorithm

The analytical results of Section 3 were obtained in the mean-field approximation, which neglects the structural heterogeneity of the network and the stochastic nature

of transitions. To verify these predictions and to quantify the effect of finite-size fluctuations, we performed a series of direct stochastic simulations of the original model described in Section 2.

The simulation proceeds in discrete time and consists of three main stages: generation of the network, initialization of node states, and iterative synchronous update of all nodes. To obtain statistically reliable estimates, each set of parameters was simulated in multiple independent runs, after which the results were averaged. The following subsections describe each stage in detail.

The network is generated as an Erdős–Rényi random graph $G(N, p)$, in which each pair of distinct nodes is connected independently with probability

$$p = \frac{\langle k \rangle}{N - 1},$$

where $\langle k \rangle$ is the target mean degree. It is known that for this model the connectivity threshold is $p_c = \ln N/N$, so that the graph is almost surely connected when $\langle k \rangle > \ln N$ [15]. For the parameter values considered in this work, this condition is satisfied with a large margin, and the probability of obtaining a connected graph is close to unity. Graphs that are not connected are rejected, and the generation is repeated until a connected graph is obtained; this rejection procedure is computationally efficient and preserves the statistical properties of the Erdős–Rényi ensemble.

We note that the actual mean degree of the generated graph, $\bar{k} = 2|L|/N$, may slightly deviate from the target value $\langle k \rangle$. In the simulations, the actual value $\bar{k}$ is used wherever a specific mean degree is required.

At the beginning of each simulation, all nodes are assigned to the disabled susceptible state (D, S). Then, choosing nodes uniformly at random without replacement:

- E_0 nodes are switched to the enabled susceptible state (E, S);
- EI_0 of the enabled nodes are switched to the enabled infected state (E, I);
- DI_0 of the remaining disabled nodes are switched to the disabled infected state (D, I).

The parameters E_0, EI_0, and DI_0 satisfy the constraints

$$0 \le E_0 \le N, \quad 0 \le EI_0 \le E_0, \quad 0 \le DI_0 \le N - E_0.$$

At each time step, all nodes update their states simultaneously. For every node i, the following procedure is applied:

1. If the node is disabled, it becomes enabled with probability λ_+.
2. If the node is enabled, it becomes disabled with probability λ_-.
3. If the node is enabled and susceptible, it becomes infected with probability μ_i given by Eq. (1), where k_i is the degree of this node. The factor $(1-\lambda_-)$ in the transition probability is implicitly accounted for by the order of operations: activity is updated first.
4. If the node is enabled and infected, it recovers with probability δ. The effective recovery probability is $(1 - \lambda_-)\delta$, following the same reasoning as for infection.

The new state of each node is computed from the configuration at the beginning of the step and stored separately. After all nodes have been processed, the new configuration replaces the old one. This synchronous update removes the dependence of the result on the order in which the nodes are traversed.

Time is discrete: $t = 0, 1, 2, \ldots, T$, where T is the total number of steps in a single realization.

The simulation consists of generating M independent Erdős–Rényi random graphs with given parameters N and $p = \langle k \rangle / (N-1)$. For each generated graph, R independent realizations of the epidemic process are performed with the same initial numbers E_0, EI_0, DI_0, but with different random assignments of nodes to the initial states. The results are averaged in two stages: first over the R realizations within each graph, and then over the M graphs. This two-level averaging accounts for two sources of randomness: the stochastic nature of transitions and the structural variability of the network.

More precisely, let $X_{g,r}(t)$ denote the value of a given quantity X at time t in the r-th realization on the g-th graph. The average over the realizations within a single graph and the ensemble average over the graphs are

$$\bar{X}_g(t) = \frac{1}{R} \sum_{r=1}^{R} X_{g,r}(t), \qquad \bar{X}(t) = \frac{1}{M} \sum_{g=1}^{M} \bar{X}_g(t).$$

In the simulations presented below, the number of realizations per graph R is chosen large enough that the contribution of the within-graph stochastic variability to the uncertainty of the ensemble mean is negligible compared with the graph-to-graph variability. The standard error is therefore estimated from the variability between the graphs alone:

$$s^2(t) = \frac{1}{M-1} \sum_{g=1}^{M} \left[\bar{X}_g(t) - \bar{X}(t) \right]^2.$$

The 95% confidence interval for the ensemble mean is

$$\bar{X}(t) \pm t_{0.975, M-1} \, \frac{s(t)}{\sqrt{M}},$$

where $t_{0.975,M-1}$ denotes the upper 2.5% point of the Student t-distribution with $M-1$ degrees of freedom.

5 Simulation Results and Comparison with Mean-Field Theory

We now compare the mean-field predictions of Section 3 with the results of direct stochastic simulations described in Section 4. The comparison is performed for several characteristic regimes, differing in the value of the basic reproduction number $\mathcal{R}_0 = \beta \langle k \rangle / \delta$.

Throughout this section, we use $N = 1000$ nodes, $M = 10$ independent graph realizations, and $R = 50$ epidemic realizations per graph, with a simulation time of $T = 500$ steps, which is sufficient for the system to reach a stationary regime in all cases considered below. The mean degree is fixed at $\langle k \rangle = 10$, which is well above the connectivity threshold $\ln N \approx 6.9$ of the Erdős–Rényi model [15], so that the generated graphs are connected with probability close to unity and the rejection procedure is computationally efficient. For simplicity, we consider the symmetric case $\lambda_+ = \lambda_- = \lambda$, so that the equilibrium fraction of enabled nodes is $e^* = 0.5$. The remaining parameters are varied to explore different regimes; their values are specified for each regime.

5.1 Limiting regimes

Before comparing the simulation results with the mean-field predictions in the general case, we first verify that the model reproduces the expected behavior in several limiting regimes. These tests serve as a consistency check of both the model formulation and its numerical implementation.

No initial infection

If the initial conditions contain no infected nodes, $EI_0 = DI_0 = 0$, no infection can appear in the system: both the mean-field equations and the simulation yield $i_E(t) = i_D(t) = 0$ for all t, and the fractions of susceptible nodes converge to the infection-free state (6). The simulation with $E_0 = 500$, $\lambda = 0.2$, and $\beta = 0.03$, $\delta = 0.1$ confirms this: $EI(t) = DI(t) = 0$ at every step, and the stationary fractions satisfy $s_D^* = s_E^* = 0.5$, in agreement with (6).

Zero transmission

Setting $\beta = 0$ prevents any transmission of the infection. Both the mean-field model and the simulation predict the extinction of the initial infection: starting with $EI_0 = 50$, the number of infected nodes decays to zero, and the system converges to the infection-free state (6). With $E_0 = 500$, $\lambda = 0.2$, and $\delta = 0.1$, the simulation gives $EI(T) \approx 0$ and $ES(T) \approx DS(T) \approx 500$, in agreement with the analytical prediction $s_E^* = s_D^* = 0.5$.

No recovery

For $\delta = 0$, infected nodes never recover, and the mean-field model predicts that the infection eventually spreads to the entire population:

$$i_E^* = s_E(0) + i_E(0) = e^* N, \quad s_E^* = 0, \quad i_D^* = (1 - e^*)N, \quad s_D^* = 0.$$

With $EI_0 = 50$, $\beta = 0.03$, and $\lambda = 0.2$, the simulation yields $EI(T) = 500.5 \pm 1.9$ and $DI(T) = 499.4 \pm 1.7$, while $ES(T)$ and $DS(T)$ are close to zero, in agreement with the analytical prediction.

Static network

As an additional reference, we consider the limiting case $\lambda_+ = \lambda_- = 0$. Since the activity state of each node is fixed, the model reduces to the classical SIS dynamics

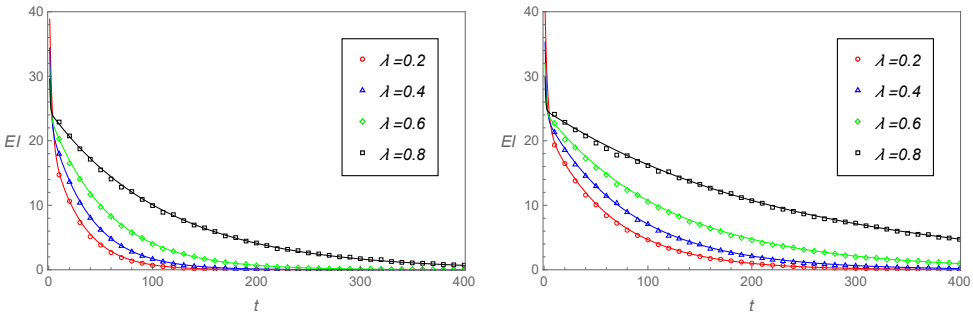

Fig. 2 Mean trajectory of the number of infected nodes $EI(t)$ for different activity rates $\lambda = 0.2, 0.4, 0.6, 0.8$. Left: subcritical regime with $\mathcal{R}_0 = 0.1$; right: $\mathcal{R}_0 = 0.6$. Points correspond to the simulation, solid curves to the mean-field solution. In both cases, increasing λ slows down the decay of the infection.

discussed in Section 3, and the exact solution (9) provides an analytical benchmark for the simulation.

For $\mathcal{R}_0 = 3$ and all nodes initially enabled, the analytical stationary fraction is $i^* = 1 - 1/\mathcal{R}_0 = 0.667$. The simulation is consistent with this prediction: the number of enabled nodes remains constant at $E(t) = 1000$, and the infected fraction converges to $EI(T) = 642 \pm 6$, compared with the analytical value $EI^* = 667$. The discrepancy of about 4% lies well outside the 95% confidence interval and therefore reflects a systematic difference between the mean-field approximation and the stochastic process, rather than statistical uncertainty. It arises from the mean-field averaging of the infection probability over the degree distribution and from finite-size effects.

5.2 General regimes

Having verified the model in the limiting cases, we now turn to the general regimes with dynamic node activity and non-degenerate parameters. We consider the subcritical, critical, and supercritical regimes separately, focusing on the effect of the activity parameter λ on the dynamics of the infection.

Subcritical regime

To study the effect of node activity on the subcritical dynamics, we consider two values of the basic reproduction number, $\mathcal{R}_0 = 0.1$ and $\mathcal{R}_0 = 0.6$, and vary the activity parameter λ over the range $\{0.2, 0.4, 0.6, 0.8\}$. In both cases we fix $\delta = 0.1$, so that the required infection probabilities are $\beta = 0.001$ for $\mathcal{R}_0 = 0.1$ and $\beta = 0.006$ for $\mathcal{R}_0 = 0.6$, according to $\mathcal{R}_0 = \beta\langle k\rangle/\delta$. The initial conditions are $E_0 = 500$ and $EI_0 = 50$. The resulting mean trajectories of infected nodes $EI(t)$ are shown in Fig. 2.

In all cases the infection level decays to zero, consistent with the theoretical prediction for $\mathcal{R}_0 < 1$. The simulations were performed up to $T = 500$; in the figures, the time range is restricted to $0 \le t \le 400$ for readability. The decay is exponential, $EI(t) \sim e^{-rt}$, and occurs faster for $\mathcal{R}_0 = 0.1$ than for $\mathcal{R}_0 = 0.6$, as expected from the distance to the epidemic threshold. The effect of the activity parameter is less intuitive: increasing λ slows down the decay. This behavior is consistent with the

interpretation that recovery is possible only for active nodes: at large λ, infected nodes spend most of their time in the disabled state, where they cannot recover, and thus act as a reservoir that sustains the infection over longer times. We also note the good agreement between the simulation and the mean-field predictions.

The observed dependence of the decay rate on λ can be understood from the linearized mean-field analysis. Linearizing the system (2)–(5) around the infection-free state for small deviations yields the decay rate

$$r(\lambda) = \frac{1}{2}\Big(2\lambda + a(1-\lambda) - \sqrt{4\lambda^2 + a^2(1-\lambda)^2}\Big), \qquad a = \delta(1-\mathcal{R}_0).$$

In the range of λ considered here ($0.2 \le \lambda \le 0.8$), this expression decreases monotonically with λ, in agreement with the simulations. This confirms that the slowdown of the decay at large λ is a direct consequence of the fact that recovery is possible only for active nodes.

Supercritical regime

In the supercritical regime, $\mathcal{R}_0 > 1$, the mean-field analysis predicts the existence of a stable endemic state, in which a finite fraction of enabled nodes remains infected (7)–(8). In the symmetric case $\lambda_+ = \lambda_- = \lambda$, the stationary number of infected nodes takes the form

$$EI^* = \frac{N}{2}\left(1 - \frac{1}{\mathcal{R}_0}\right).$$

Notably, this expression does not depend on the activity parameter λ: the stationary level of infection is determined solely by the distance from the epidemic threshold, whereas the activity parameters affect only the fraction of enabled nodes.

To verify the mean-field prediction and to study the effect of the activity parameter on the dynamics, we performed a series of simulations for two values of the basic reproduction number, $\mathcal{R}_0 = 3$ and $\mathcal{R}_0 = 5$, varying the activity parameter λ over the range $\lambda \in \{0.2, 0.4, 0.6, 0.8\}$. In both cases we fix $\delta = 0.1$, so that the required infection probabilities are $\beta = 0.03$ for $\mathcal{R}_0 = 3$ and $\beta = 0.05$ for $\mathcal{R}_0 = 5$, according to $\mathcal{R}_0 = \beta\langle k\rangle/\delta$. The initial conditions are $E_0 = 500$ and $EI_0 = 50$. The resulting mean trajectories of infected nodes $EI(t)$ are shown in Fig. 3.

The initial stage of the dynamics is not monotonic for large λ: after a short transient, during which $EI(t)$ decreases, the curves grow and approach a stationary plateau. The depth of this initial dip increases with λ. For example, at $\mathcal{R}_0 = 5$, the value of EI at $t = 10$ grows to 160 for $\lambda = 0.2$, but decreases to 38 for $\lambda = 0.8$ before the infection starts to spread. This behavior reflects the competition between fast activity switching and slower infection transmission: at large λ, infected nodes spend more time in the disabled state, where they cannot transmit the infection.

After the transient, all curves converge to the same stationary plateau, which depends only on $\mathcal{R}_0$ and not on λ. For $\mathcal{R}_0 = 3$, the plateau is $EI^* \approx 320$ (mean-field: 333); for $\mathcal{R}_0 = 5$, it is $EI^* \approx 390$ (mean-field: 400). In both cases, the simulation results are systematically slightly below the analytical prediction.

The time required to reach the plateau increases with λ. For $\mathcal{R}_0 = 5$, the stationary level is reached by $t \approx 50$ at $\lambda = 0.2$ and only by $t \approx 250$ at $\lambda = 0.8$. For $\mathcal{R}_0 = 3$, the

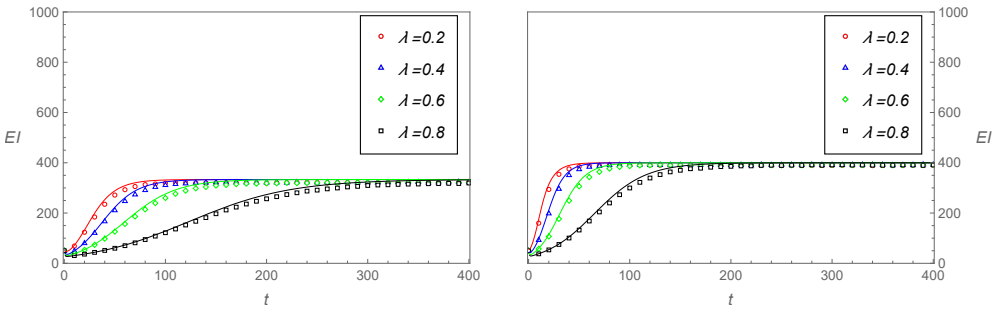

Fig. 3 Mean trajectory of the number of infected nodes $EI(t)$ for different activity rates $\lambda = 0.2, 0.4, 0.6, 0.8$. Left: supercritical regime with $\mathcal{R}_0 = 3$; right: $\mathcal{R}_0 = 5$. Points correspond to the simulation, solid curves to the mean-field solution.

corresponding times are $t \approx 100$ and $t \approx 400$. This slowdown is consistent with the behavior observed in the subcritical regime, where the decay rate was also found to decrease with increasing λ.

To verify the mean-field prediction for the stationary state, we extracted the plateau values $EI(T)$ at $T = 400$ for each value of λ and both values of $\mathcal{R}_0$. The resulting stationary levels are summarized in Table 1.

Table 1 Stationary number of infected nodes EI^* for different activity rates λ and two values of the basic reproduction number $\mathcal{R}_0$. The remaining parameters are fixed at $\delta = 0.1$, $E_0 = 500$, and $EI_0 = 50$. The last row shows the mean-field prediction.

	$\mathcal{R}_0 = 3$ ($\beta = 0.03$)					$\mathcal{R}_0 = 5$ ($\beta = 0.05$)				
λ	0.1	0.3	0.5	0.7	0.9	0.1	0.3	0.5	0.7	0.9
EI^*	321.7	319.7	319.4	321.0	320.6	391.4	389.9	389.2	391.5	390.9
$\pm$	2.0	2.7	2.0	2.2	1.4	1.4	1.9	1.5	1.9	1.7
Mean-field ($\mathcal{R}_0 = 3$): $EI^* = 333.3$						Mean-field ($\mathcal{R}_0 = 5$): $EI^* = 400.0$				

Two observations follow from Table 1. First, the stationary level EI^* is essentially independent of the activity parameter λ. For $\mathcal{R}_0 = 3$, the values vary between 319.4 and 321.7, with an overall spread of less than 1%. For $\mathcal{R}_0 = 5$, the spread is similarly small. This is in agreement with the mean-field prediction, which yields $EI^* = 1 - 1/\mathcal{R}_0$ independently of λ. Second, the simulation results are systematically below the analytical prediction, by about 3.7% for $\mathcal{R}_0 = 3$ and 2.3% for $\mathcal{R}_0 = 5$. This discrepancy is much larger than the confidence intervals and therefore reflects a systematic effect rather than statistical uncertainty. It arises from the mean-field averaging of the infection probability over the degree distribution: in the simulation, the infection probability of each node depends on its individual degree k_i, whereas the mean-field model uses the average degree $\langle k \rangle$.

Notably, the relative discrepancy decreases with increasing $\mathcal{R}_0$, consistent with the fact that the mean-field approximation becomes more accurate far from the epidemic threshold.

Conclusion

In this work, we studied the spread of malicious software in a computer network with dynamic node activity. The central question was whether the classical epidemic threshold of the SIS model is preserved in the presence of time-varying activity, and how the activity parameter λ affects the dynamics of the infection. To address this question, we developed a stochastic model in which each node is characterized by an activity state and an epidemiological state, derived its mean-field analogue, and compared the analytical predictions with direct stochastic simulations.

The main results can be summarized as follows. First, the epidemic threshold is preserved in the presence of dynamic activity: the mean-field analysis yields $\mathcal{R}_0 = \beta\langle k\rangle/\delta$, independently of the activity parameters, in agreement with the classical SIS result and with the simulations. Second, the stationary state is also independent of the activity parameter: in the supercritical regime, the stationary number of infected nodes depends only on $\mathcal{R}_0$, while λ affects the fraction of enabled nodes but not the relative infection level within the enabled subpopulation. Third, the activity parameter strongly affects the transient dynamics. In the subcritical regime, increasing λ slows down the decay of the infection; a similar slowdown is observed in the supercritical regime for the convergence to the stationary state. This counterintuitive behavior is explained by the fact that recovery is possible only for active nodes: at large λ, infected nodes spend most of their time in the disabled state, where they cannot recover, and thus act as a reservoir that sustains the infection over longer times. The analytical expression for the decay rate, obtained from the linearized mean-field equations, reproduces this behavior quantitatively.

The main limitations of this study are the mean-field approximation, which neglects the structural heterogeneity of the network; the restriction to Erdős–Rényi graphs and to the symmetric case $\lambda_+ = \lambda_-$; and the linearization of the infection probability, which is valid only for $\beta i\langle k\rangle \ll 1$. The critical regime $\mathcal{R}_0 \approx 1$ was not studied in detail because of the slow convergence and strong finite-size effects.

Possible directions for future research include the extension of the model to other network topologies, the use of the exact infection probability, the analysis of asymmetric activity rates, and the study of the critical regime with longer simulations and larger system sizes. We also plan to explore the non-monotonic dependence of the decay rate on λ observed in the linearized analysis, which may have implications for the design of activity-based interventions.

Declarations

Funding. The research of A. A. Magazev was carried out within the state assignment of the Ministry of Science and Higher Education of the Russian Federation (theme No. FSGF-2026-0003).

Conflict of interest. The authors declare that they have no conflict of interest.

Ethics approval and consent to participate. Not applicable.

Consent for publication. Not applicable.

Data availability. The data generated during this study are included in this article.

Materials availability. Not applicable.

Code availability. The simulation code used in this study is available from the corresponding author on reasonable request.

Author contribution. A. V. Nikiforov: software, numerical simulations, data analysis. A. A. Magazev: conceptualization, methodology, writing, supervision. All authors read and approved the final manuscript.

References

[1] Pastor-Satorras, R., Castellano, C., Van Mieghem, P., Vespignani, A.: Epidemic processes in complex networks. Reviews of modern physics **87**(3), 925–979 (2015) https://doi.org/10.1103/RevModPhys.87.925

[2] Karmaker, C.L., Al Aziz, R., Arman, M.H., Zhuang, J.: A systematic review of controlling rumors in online social networks: Insights from epidemiological models. Risk Analysis **46**(5), 70247 (2026) https://doi.org/10.1111/risa.70247

[3] Raponi, S., Khalifa, Z., Oligeri, G., Di Pietro, R.: Fake news propagation: A review of epidemic models, datasets, and insights. ACM Transactions on the Web (TWEB) **16**(3), 1–34 (2022) https://doi.org/10.1145/3522756

[4] Prakash, O., Kumar, A.: Computer virus propagation models: A mathematical review. In: 2025 3rd International Conference on Communication, Security, and Artificial Intelligence (ICCSAI), vol. 3, pp. 1–5 (2025). https://doi.org/10.1109/ICCSAI64074.2025.11064109

[5] Duan, D., Yang, X., Lv, C., Cai, Z.: Modeling and predicting malware propagation in double-layer computer networks. IEEE Transactions on Network Science and Engineering **13**, 717–727 (2026) https://doi.org/10.1109/TNSE.2025.3586909

[6] Centola, D.: The spread of behavior in an online social network experiment. science **329**(5996), 1194–1197 (2010) https://doi.org/10.1126/science.1185231

[7] Goel, S., Anderson, A., Hofman, J., Watts, D.J.: The structural virality of online diffusion. Management science **62**(1), 180–196 (2016) https://doi.org/10.1287/mnsc.2015.2158

[8] Albert, R., Barabási, A.-L.: Statistical mechanics of complex networks. Reviews of modern physics **74**(1), 47 (2002)

[9] Holme, P., Saramäki, J.: Temporal networks. Physics Reports **519**(3), 97–125 (2012) https://doi.org/10.1016/j.physrep.2012.03.001

[10] Perra, N., Gonçalves, B., Pastor-Satorras, R., Vespignani, A.: Activity driven modeling of time varying networks. Scientific Reports **2**, 469 (2012) https://doi.org/10.1038/srep00469

[11] Kephart, J.O., White, S.R.: Directed-graph epidemiological models of computer viruses. In: Proceedings of the 1991 IEEE Computer Society Symposium on Research in Security and Privacy, pp. 343–359. IEEE Computer Society Press, Los Alamitos, CA (1991). https://doi.org/10.1109/RISP.1991.130801

[12] Billings, L., Spears, W.M., Schwartz, I.B.: A unified prediction of computer virus spread in connected networks. Physics Letters A **297**(3–4), 261–266 (2002) https://doi.org/10.1016/S0375-9601(02)00152-4

[13] Magazev, A.A., Nikiforova, A.Y.: On the applicability of a markov virus spread model to e-mail graphs. In: 2023 Dynamics of Systems, Mechanisms and Machines (Dynamics), pp. 1–4 (2023). https://doi.org/10.1109/Dynamics60586.2023.10349374

[14] Pastor-Satorras, R., Vespignani, A.: Epidemic spreading in scale-free networks. Physical Review Letters **86**(14), 3200–3203 (2001) https://doi.org/10.1103/PhysRevLett.86.3200

[15] Bollobás, B.: Random Graphs, 2nd edn. Cambridge Studies in Advanced Mathematics, vol. 73. Cambridge University Press, Cambridge (2001). https://doi.org/10.1017/CBO9780511814068